Agricultural and Forest Meteorology 185 (2014) 1–13

Contents lists available at ScienceDirect

Agricultural and Forest Meteorology

journal homepage: www.elsevier.com/locate/agrformet

Inferring the contribution of advection to total ecosystem scalar fluxes over a tall forest in complex terrain

K. Novick[a,*], S. Brantley[b,c], C. Ford Miniat[b], J. Walker[d], J.M. Vose[e]

[a] School of Public and Environmental Affairs, Indiana University – Bloomington, 1315 E 10th Street, Bloomington, IN 47405, United States
[b] USDA Forest Service – Southern Research Station – Coweeta Hydrologic Laboratory, 3160 Coweeta Lab Road, Otto, NC 2873, United States
[c] Department of Forest Resources, University of Minnesota, 530 Cleveland Ave. N., St. Paul, MN 55108, United States
[d] US EPA National Risk Management Research Laboratory, 109 T.W. Alexander Dr., Mail Drop E305-02, RTP, NC 2771, United States
[e] USDA Forest Service – Southern Research Station – Center for Integrated Forest Science, North Carolina State University, Department of Forestry and Environmental Resources, Campus Box 8008, Raleigh, NC 27695-8008, United States

ARTICLE INFO

Article history:
Received 5 July 2013
Received in revised form 18 October 2013
Accepted 21 October 2013

Keywords:
Eddy covariance
Complex terrain
Advection
Sap flux
Carbon flux
Energy balance

ABSTRACT

Multiple data streams from a new flux tower located in complex and heterogeneous terrain at the Coweeta Hydrologic Laboratory (North Carolina, USA) were integrated to identify periods of advective flow regimes. Drainage flows were expected a priori, due to the location of the measurement site at the base of a long, gently-sloping valley. Drainage flow was confirmed by examining vertical profile measurements of wind direction and by estimating vertical advection fluxes. The vertical advection flux of CO_2 was most significant in early morning (000–0600 h) during the growing season, when it averaged $\sim$5 μmol m^{-2} s^{-1}. Horizontal advection flux of CO_2 was not directly measured in this study; however, an expected exponential relationship between nocturnal ecosystem respiration (RE) and air temperature was recovered when horizontal advection of CO_2 was assumed to be negatively correlated to vertical advection, or when data were limited to periods when measured vertical advection fluxes were small. Taken together, these data imply the presence of a negative horizontal advection CO_2 flux during nocturnal periods characterized by positive vertical advection of CO_2. Daytime periods were characterized by consistent anabatic (up-valley) flows in mid- to late-morning (0500–1200 h) and consistent katabatic (down-valley) flows in the afternoon. A combination of above-canopy flux profile measurements, energy balance closure estimates, and flux footprint estimates suggest that during periods of up-valley wind flow, the flux footprint frequently exceeds the ecosystem dimensions, and horizontal advection fluxes related to landscape heterogeneity were a significant component of the total ecosystem flux of CO_2. We used sap flux from individual trees beneath the tower to explore diurnal patterns in stomatal conductance in order to evaluate gapfilling approaches for the unreliable morning data. The relationship between stomatal conductance and vapor pressure deficit was similar in morning and afternoon periods, and we conclude that gapfilling morning data with models driven by afternoon data is a reasonable approach at this site. In general, results were consistent with other studies showing that the advection and wind flow regimes in complex terrain are highly site specific; nonetheless, the site characterization strategy developed here, when used together with independent estimates of components of the ecosystem carbon flux, could be generally applied in other sites to better understand the contribution of advection to the total ecosystem flux.

1. Introduction

The eddy covariance technique permits quasi-continuous monitoring of biosphere-atmosphere scalar fluxes directly at the ecosystem scale for long periods of time (Baldocchi, 2008; Friend et al., 2007). In most applications, the net ecosystem flux of the scalar of interest is linked to the vertical turbulent flux measured above the canopy and a storage flux estimate derived from the temporal change in within-canopy scalar concentration (Aubinet, 2008; Baldocchi, 2003). Turbulent and storage fluxes may be observed from a single measurement tower, promoting the development of an extensive network of more than 400 flux monitoring towers across a range of biomes (Baldocchi, 2008). Collectively, these data have promoted significant knowledge advancements related to the process-based controls on ecosystem carbon and water cycling and dynamic interactions between the biosphere and the atmosphere (Baldocchi, 2008; Falge et al., 2002; Friend et al., 2007; Krinner et al., 2005; Law et al., 2002; Williams et al., 2009). However, due

* Corresponding author. Tel.: +1 812 855 3010.
E-mail address: knovick@indiana.edu (K. Novick).

0168-1923/$ – see front matter © 2013 Elsevier B.V. All rights reserved.
http://dx.doi.org/10.1016/j.agrformet.2013.10.010

to methodological challenges that complicate the interpretation of data collected from heterogeneous or complex terrain, the network has historically been biased toward flat, homogeneous sites. Following a brief review of the theory governing the interpretation of data from eddy covariance flux towers, we discuss these challenges and outline an approach for characterizing fluxes in heterogeneous and complex terrain relying on data collected from a single tower.

Following Feigenwinter et al. (2010a), and assuming negligible horizontal flux divergence, the total flux of a scalar from an ecosystem (F_S) may be expressed as:

$$F_S = \underbrace{\int_0^L \int_0^L \int_0^{z_r} \frac{\partial \overline{\rho_S(z)}}{\partial t} dz}_{\text{Term I}} + \underbrace{\overline{w'\rho'_S}(z_r)}_{\text{Term II}} + \underbrace{\int_0^{z_r} \overline{w(z)} \frac{\partial \overline{\rho_S(z)}}{\partial z} dz}_{\text{Term III}} + \underbrace{\frac{1}{4L^2} \int_{-L}^{L} \int_{-L}^{L} \int_0^h \left(\frac{\overline{u(z)} \partial \overline{\rho_S(z)}}{\partial x} + \frac{\overline{v(z)} \partial \overline{\rho_S(z)}}{\partial y} \right)}_{\text{Term IV}} \quad (1)$$

where u, v, and w represent wind speeds in the x, y, and z directions, respectively, ρ_s is the mass density of the scalar, and z_r is the flux measurement height and the height of a representative control volume over which F_S is calculated. The variable L represents the length of the sides of the control volume, and h is the canopy height. The first term on the right hand side (Term I) represents the storage flux, or the change in concentration with time, integrated from $z = 0$ to z_r. This storage flux is negligible over daily and longer time-scales; at finer temporal resolutions, it may be estimated from vertical profile measurements of CO_2. Term II represents the vertical turbulent flux, which may be measured using the eddy covariance technique with a sonic anemometer and fast-response gas analyzer co-located above the canopy. Term III represents the vertical advection of the scalar into or out of the control volume by a non-zero mean vertical wind velocity ($\overline{w(z)}$). In most cases, $\overline{w(z)}$ is assumed to be zero, such that vertical advection of the scalar is also assumed to be zero; however, estimates of the vertical advection flux occurring during periods of non-negligible $\overline{w(z)}$ can be derived from scalar profile measurements and wind profile measurements on a single tower (Lee, 1998; Leuning et al., 2008). Term IV represents the horizontal advection of the scalar into or out of the control volume, generated primarily by horizontal gradients in scalar source intensity or surface roughness (Baldocchi et al., 1999). Horizontal advection is difficult to measure and requires an array of towers (Aubinet et al., 2010; Feigenwinter et al., 2008). In most sites, the land surface around the tower is usually assumed to be horizontally homogeneous, such that horizontal advection fluxes are also negligible. With these assumptions, F_S reduces to the sum of the vertical turbulent flux (Term II), which may be augmented by storage flux estimates (Term I) at hourly time scales.

The interpretation of the sum of vertical turbulent fluxes and storage fluxes as representative of the total ecosystem flux is challenged whenever the assumptions of negligible vertical and horizontal advection (i.e., Terms III and IV), or negligible horizontal flux divergence, are invalidated. The contribution of advection fluxes to the total ecosystem flux is likely greatest in (a) heterogeneous sites where horizontal advection is driven by scalar gradients associated with land cover transitions, and (b) sites characterized by complex topography where vertical wind speed is often non-negligible and elevation gradients produce horizontal gradients in wind and scalar fields.

A growing number of flux monitoring sites are situated in complex or heterogeneous terrain (Baldocchi et al., 2000; Feigenwinter et al., 2008; Gockede et al., 2004; Kutsch et al., 2008; Rebmann et al., 2005; Yi et al., 2005). Furthermore, a growing body of work suggests that advection may often be non-negligible even in relatively 'flat' sites (Feigenwinter et al., 2010a; van Gorsel et al., 2009; Loescher et al., 2006), where even a small vertical wind speed superimposed over a large vertical scalar gradient can produce a significant vertical advection flux. In some experiments, multiple observation towers have been erected to quantify both horizontal and vertical advection fluxes (Staebler and Fitzjarrald, 2004; Sun et al., 2007); in general, results from these studies show that the advection flux regime is highly site specific (Aubinet et al., 2010; Yi et al., 2008), and that the advection flux estimates themselves are characterized by a high level of uncertainty (Aubinet et al., 2010; Loescher et al., 2006). Given these results, and that the cost of erecting multiple above-canopy observation towers is often prohibitive, a multi-tower experimental design may not be a practical approach for accurately measuring advection fluxes. However, knowledge gained from these advection studies, taken together with techniques for estimating vertical advection from a single tower (Lee, 1998; Leuning et al., 2008) and an improved understanding of the components of ecosystem energy balance (Foken, 2008; Lindroth et al., 2010; Wilson et al., 2002) may permit the identification of flux measurements collected during periods when advection is significant (Loescher et al., 2006), even if the magnitude of the advection fluxes is not known with certainty. These data could then be removed from the data records and gapfilled according to a number of established approaches (Reichstein et al., 2005; van Gorsel et al., 2009) that may be augmented with independent biometric observations.

In this study, we applied such a framework in a new eddy covariance site located in heterogeneous and complex terrain near the Coweeta Hydrologic Laboratory in western NC, USA. We used a comprehensive suite of observations collected from a single tower to answer the following question: *Can periods characterized by significant horizontal and vertical advection be identified with observations from a single flux tower, even if the magnitude of their sum is not known?* Specifically, our analysis relied on the following observations and approaches:

(1) Characterization of within- and above-canopy wind flows focused on the occurrence of non-negligible vertical wind speed (a necessary condition for vertical advection) and within-canopy divergence in wind direction (which could indicate a decoupling between above- and below-canopy wind flows).
(2) Characterization of the flux footprint to identify periods when the footprint exceeds the dimensions of the study system, or when land cover heterogeneity near the edge of the footprint may contribute to horizontal advection.
(3) Exploration of vertical advection fluxes determined from observations of the vertical profile of the scalars.
(4) Evaluation of the divergence between fluxes measured at two heights above the canopy, noting that if fluxes measured at two points in the constant flux layer agreed (after correction for differences in storage), then the sum of horizontal and vertical advection fluxes was likely near zero (Baldocchi et al., 2000, Yi et al., 2000), unless horizontal advection was confined to the lower canopy.
(5) Evaluation of the energy balance closure for various wind regimes, noting that poor energy balance closure could indicate significant advection fluxes of latent or sensible heat (Foken, 2008).
(6) Comparison of the carbon fluxes measured above the canopy and in the sub-canopy. At night, the above-canopy fluxes should be greater than sub-canopy fluxes reflecting the contribution of above-ground autotrophic respiration to total ecosystem respiration; however, the ratio of above- to below-canopy carbon fluxes may be decreased if much of the respiration flux is carried away by horizontal advection in the canopy airspace.

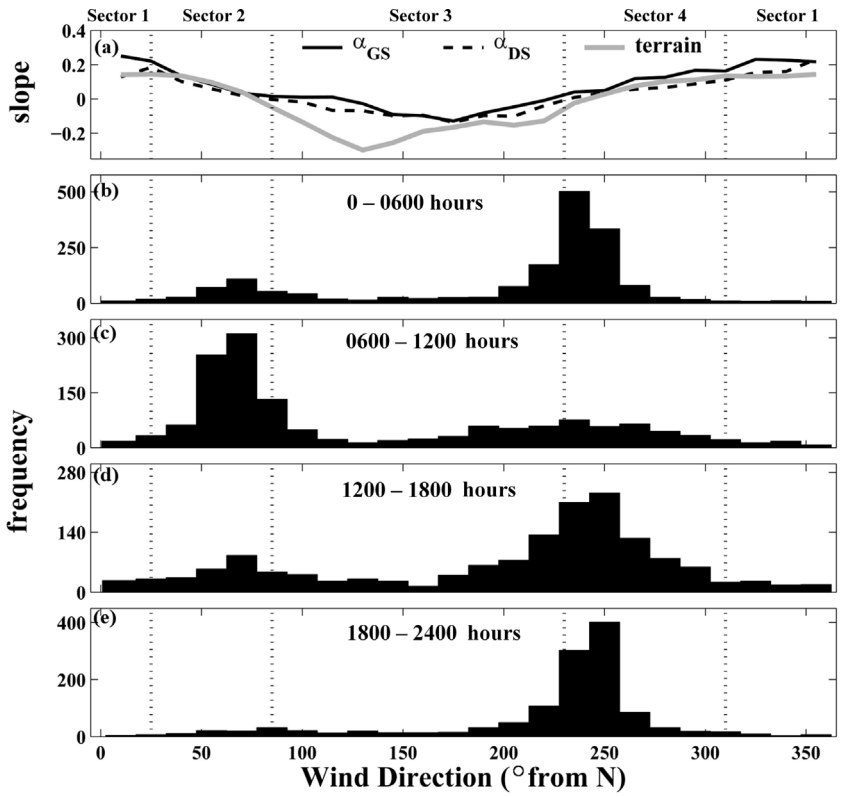

Fig. 1. Wind flow characteristics in the vicinity of the flux tower. The wind angle of attack during both the growing and dormant season (α_{GS} and α_{DS}, respectively) was closely aligned with the slope of the local terrain (panel a). The wind direction histograms in (b)–(e) show that wind direction was predominantly from the E-NE (i.e., Sector 2) in morning periods, and from the W-SW (i.e., Sector 4) otherwise.

(7) Exploration of the temperature dependencies of the nocturnal CO_2 fluxes, which represent ecosystem respiration (RE). A failure to observe an exponential relationship between RE and temperature, which has been widely reported for many ecosystems (Reichstein et al., 2003; Reichstein and Beer, 2008; Vose and Bolstad, 2006; Schmid et al., 2000), could indicate a significant contribution from an unmeasured advection flux or horizontal flux divergence.

2. Methods

2.1. Study site

The experiment was conducted in a ~80 year-old mixed hardwood forest (35.059 N, 83.427 W, 690 m a.s.l.) in the Coweeta Hydrologic Laboratory. Coweeta is located in the southern Appalachian Mountains of western North Carolina and is a USDA Forest Service Experimental Forest and National Science Foundation Long-Term Ecological Research Site. The tower is situated in complex, mountainous terrain characterized by a 30% slope within the flux footprint in the SE direction, and local slopes of <10% to the NE and SW (Fig. 1). Mean annual temperature is 12.9 °C and mean annual precipitation is 1795 mm. Dominant canopy species near the tower are *Liriodendron tulipifera* L. (Magnoliaceae), *Quercus alba* L. (Fagaceae), *Betula lenta* L. (Betulaceae), and *Acer rubrum* L. (Aceraceae), which comprise 24%, 17%, 11% and 8% of the basal area, respectively. The dominant sub canopy species is *Rhododendron maximum* L. (Ericaceae), which comprises 13% of basal area. Peak growing season leaf area, measured with a LAI-2000 plant canopy analyzer (Li-COR Biosciences, Lincoln, NE), was ~5.8 $m^2\ m^{-2}$. Mean canopy height (h) was ~30 m, and basal area was 28.9 $m^2\ ha^{-1}$.

2.2. Turbulent eddy covariance flux measurement and processing

Long-term eddy covariance (EC) measurements were made with an infrared gas analyzer (EC155, Campbell Scientific, Logan, Utah) and a sonic anemometer (RM-Young 81000; RM Young, Traverse City, MI, USA) co-located at a height of 37 m. The inlet of the EC155 was separated from the sonic at a lateral distance of approximately 10 cm, and each instrument was supported with a dedicated pole (see Fig. 2). Raw data were collected and stored at 10 Hz on the same CR-3000 datalogger (Campbell Scientific), with both the EC155 and RM-Young instruments sharing the same SDM communication channels. Data were post-processed into hourly averages after adjusting the gas analyzer and sonic anemometer time series to

Fig. 2. The EC155 and RM Young 81000 sonic anemometer, positioned at a height of z = 37 m above the canopy.

account for a 0.2 s lag between the two data records. Coordinate axes of the wind data were rotated using a sector-wise planar-fit (Wilczak et al., 2001) approach, with sectors delineated as follows: (1) Sector 1, wind direction (WD) <40° or >310° clockwise from N, (2) Sector 2, WD between 40° and 85° from N, (3) Sector 3, WD between 86° and 229° from N, and (4) Sector 4, WD between 230° and 310° from N (Fig. 1). These sectors were informed by the relationship between the local topographic slope and the wind angle of attack determined from the sonic anemometer data after a 1-D coordinate rotation to align horizontal wind speed with the mean wind direction. For wind Sectors 2 and 4, the angle of attack was closely aligned with the topography (Fig. 1a); thus, a planar fit rotation should produce effective streamline coordinates when wind originates from Sectors 2 and 4. When wind originates from Sectors 1 and 3, the angle of attack and the slope angle diverged considerably for Sectors 1 and 3 (Fig. 1a); thus, fluxes are expected to be unreliable a priori when wind originates from these directions, which we note represent a small fraction of the flux measurements (Fig. 1b–e). Hourly-averaged horizontal and vertical wind speed components after the planar fit rotation are denoted as $\overline{u(z)}$ and $\overline{w(z)}$, respectively. The sonic was oriented to 220° from N, and the analyzer inlet is located northeast of the sonic.

All variables were detrended before calculation of means and turbulent fluxes, and fluxes were calculated for hourly averaging periods. As described in Novick et al. (2013), carbon and water vapor fluxes were calculated directly from the mixing ratio measured with the EC155. Sensible heat flux (H) was calculated using virtual temperature measurements from the sonic anemometer corrected for water vapor concentration to an estimate of actual air temperature. An analytical spectral correction (Massman, 2000, 2001) was applied to the flux data as described in Novick et al. (2013). Latent heat flux (LE) was determined from water vapor fluxes using the temperature-dependent latent heat of vaporization. The turbulent fluxes are denoted as $F_{C,EC}$, LE_{EC}, and H_{EC} for carbon, latent heat, and sensible heat fluxes, respectively

For some portions of this analysis, data were limited to those collected when friction velocity (u^*) was relatively high ($u^* > 0.25\ m\ s^{-1}$) to determine to what extent features of the flux data were related to low or insufficient turbulence. Similarly, some analysis was limited to data collected when u^* was low ($<0.1\ m\ s^{-1}$) to better elucidate patterns in vertical advection and storage fluxes, which are greatest when turbulent mixing is low. When these filters have been applied, a note will be made in the text. Turbulent flux data were collected for almost a full year (January to December, 2011).

2.3. Storage & vertical advection fluxes

Storage fluxes (i.e., Term I of Eq. (1)) were estimated by integrating temporal changes in CO_2, H_2O, and air temperature (T_a) in the vertical direction, using profile measurements of the scalars at heights of 4, 9, 16, 24, 30, and 37 m. The vertical CO_2 and H_2O profiles were measured using a closed-path infrared gas analyzer (LI-840; Li-COR, Lincoln, NE, USA) that switched between measurement heights once every minute using a multiplexer and data acquisition system designed by Campbell Scientific; the system is a prototype for the AP200 CO_2/H_2O Atmospheric Profile System (Campbell Scientific). Tube lengths were roughly the same as the inlet location heights, as the analyzer and datalogger were housed in an enclosure mounted to the base of the tower. Sample flow rate was set to ~110 mL/min, and sample pressure was held constant at 50 kPa. Data were collected at 5 Hz and post-processed into hourly averages. The vertical temperature gradients were measured with a profile of aspirated thermocouples. The storage fluxes are denoted as $F_{C,STOR}$, LE_{STOR}, and H_{STOR} for carbon, latent heat, and sensible heat fluxes, respectively.

Vertical advection fluxes were calculated after Leuning et al. (2008) as:

$$F_{VA} = \overline{w(z)}\left(\overline{\rho_S(z)} - \frac{\int_0^{z_r}\overline{\rho_S(z)}S(z)dz}{\int_0^{z_r}\overline{S(z)}dz}\right), \quad (2)$$

where $S(z)$ is the normalized horizontal wind speed (i.e., $\overline{u(z)}/\overline{u(z_r)}$) and the vertical scalar profiles (i.e., $\rho_S(z)$) are measured with the profile systems described above. The vertical advection fluxes are denoted as $F_{C,VA}$, LE_{VA}, and H_{VA} for carbon, latent heat, and sensible heat fluxes, respectively. Relatedly, the total ecosystem fluxes of carbon, latent heat, and sensible heat are denoted as F_C, LE, and H. These total fluxes are equivalent to the sum of measured turbulent fluxes, storage fluxes, vertical advection flux, and horizontal advection flux and flux divergence; Again, the horizontal advection and flux divergence were not directly measured in this study. The sum of turbulent, storage, and vertical advection fluxes are denoted as F_C^*, LE^*, and H^*; these fluxes should be interpreted as the total ecosystem flux less the contribution from horizontal advection and horizontal flux divergence.

2.4. Vertical flux profile

From August 2011 to December 2011, a temporary flux profile comprised of two open-path EC systems was installed above the canopy (at heights of 33 and 37 m). These systems were comprised of an open-path infrared gas analyzer (LI-7500) and a sonic anemometer (RM-Young 81000). Similar to the permanent EC system, data were collected at 10-Hz and processed into hourly averages. Wind measurements were rotated using the same sector-wise, planar-fit approach described in Section 2.2. Variables were de-trended and CO_2 and H_2O fluxes were calculated from mass density concentration measurements. Terms accounting for fluctuations in air density (Webb et al., 1980) were added to the fluxes, and the Massman (2000, 2001) spectral correction were also applied to the open-path data records. More details about the processing of data from these open path systems are given in Novick et al., 2013.

2.5. Footprint

The flux footprint was determined for some portions of the study period at a 5 m spatial resolution using the 2-D footprint model of Detto et al. (2006), which is an adaptation of the analytical footprint model of Hsieh et al. (2000) to include lateral dispersion. Specifically, the flux footprint was calculated for 100 daytime measurement periods during the growing season when wind was from Sector 2, for 100 daytime measurement periods during the growing season when wind was from Sector 4, and for 100 nocturnal measurement periods during the growing season when the wind was from Sector 4. In each case, the footprints were summed and normalized by 100 such that a value of 1.0 for a particular grid cell indicates that 100% of the footprint estimates overlaid the cell. The normalized frequency distributions were then superimposed on high-resolution aerial photography images (USGS 1:24000 Digital orthophoto quadrangles).

2.6. Energy balance measurements

Consideration of thermodynamic principles requires that the sum of latent and sensible heat fluxes (LE and H, respectively) should be equivalent to the difference between net radiation (R_n)

and the sum of ground heat flux (G) and all other energy sources and sinks (Q) (Wilson et al., 2002):

$$LE + H = R_n - G - Q. \quad (3)$$

The Q term, which incorporates biomass heat storage and biochemical energy storage, is generally expected to be small, though some work shows that these fluxes may represent a significant fraction of the ecosystem energy balance (Gu et al., 2007; Lindroth et al., 2010; Moderow et al., 2009; Oncley et al., 2007). Here, Q was neglected, though the potential contribution of biomass heat storage and biochemical energy storage is discussed. R_n was measured at the top of the canopy using a 4-component net radiometer (CNR 4, Kipp & Zonen, Delft, the Netherlands), with data saved as hourly averages. G was measured by averaging the output from four soil heat flux plates (HPF01, Hukseflux, Delft, the Netherlands) deployed at a distance of 10 m in the four cardinal directions from the center of the tower. Energy balance closure was determined from the energy balance ratio (EBR, Wilson et al., 2002), which is defined as the sum of turbulent, vertical advection, and storage fluxes of latent and sensible heat normalized by available radiation:

$$EBR = \frac{LE_{EC} + LE_{STOR} + H_{EC} + H_{STOR}}{R_N - G} \quad (4)$$

Since the unmeasured horizontal advection fluxes are not included in the calculation of the EBR, an EBR that is far from 1.0 could indicate significant horizontal advection.

2.7. Eddy covariance measurements in the sub-canopy

For a portion of the study period (August–December, 2011), scalar fluxes were measured in the sub-canopy using an eddy covariance system comprised of an open-path infrared gas analyzer (LI-7500) and a sonic anemometer (RM-Young 81000) positioned at a height of 2 m and a lateral distance of 30 m from the tower. The 2-m sonic was oriented in the same direction as the 46-m sonic (i.e., 220° from N). Wind and scalar concentration data were collected and stored at 10 Hz, and fluxes were processed after applying a planar fit coordinate rotation (Wilczak et al., 2001) and appropriate spectral and air density corrections (Massman, 2000, 2001; Webb et al., 1980). Carbon fluxes measured by the sub-canopy system included forest-floor efflux as well as some fraction of vegetative carbon exchange from understory vegetation and the base of tree stems.

2.8. The temperature dependency of nocturnal carbon fluxes

The dependence of ecosystem respiration (i.e., RE) on air temperature (T_a) was assumed to take the form (Vose and Bolstad, 2006):

$$RE = b_o \exp(b_1 T_a) \quad (5)$$

where b_o is the reference respiration rate, and b_1 is a temperature sensitivity parameter. This relationship was assessed using four estimates of RE. First, RE was estimated from nocturnal F_C^* data collected when $F_{C,EC}$ was near zero ($|F_{C,EC}| < 2\ \mu mol\ m^{-2}\ s^{-1}$), such that F_C^* was dominated by $F_{C,VA}$ and $F_{C,STOR}$ (RE_1). Then, a revised RE (RE_2) was estimated by assuming that the unmeasured horizontal advection flux ($F_{C,HA}$) was positively correlated with $F_{C,VA}$ with a slope of 0.5, such that $RE_2 = F_C^* + 0.5F_{C,VA}$. RE was again estimated by assuming $F_{C,HA}$ was negatively correlated with $F_{C,VA}$ with a slope of −0.5, such that $RE_3 = F_C^* - 0.5F_{C,VA}$. These assumed values of $F_{C,HA}$ reflect results from previous studies showing that horizontal and vertical advection are often correlated and may be of similar magnitude (Aubinet et al., 2010; Yi et al., 2008; Feigenwinter et al., 2004). Because the slopes (i.e., 0.5 and −0.5) were arbitrary, the analysis was not intended to give an accurate estimate of the magnitude of RE; however, analyzing the relationship between RE and temperature under different assumptions for $F_{C,HA}$ may give at least an indication of the nature of the relationship between $F_{C,HA}$ and $F_{C,VA}$. Finally, the parameters of Eq. (5) were evaluated again, this time limiting data to those collected from sunset to midnight when $|F_{C,VA}| < 2\ \mu mol\ m^{-2}\ s^{-1}$ (RE_4). These conditions are analogous to those proposed by van Gorsel et al. (2009) for a data filtering and gapfilling approach designed to minimize the contribution of advection. Under these conditions, RE_4 should be dominated by $F_{C,EC}$ and $F_{C,STOR}$. In all cases, the parameters of Eq. (5) were determined using binned averages of T_a and RE.

2.9. Sap flux measurements

Temporal trends in stomatal conductance derived from sap flux measurements were used in this study to inform an assessment of how advection regimes will affect future efforts to gapfill and partition measured fluxes. We installed constant heat thermal dissipation sensors (Granier, 1985) in the vicinity of the tower to determine sap flux density (J_s, $g\ H_2O\ m^{-2}$ sapwood s^{-1}) in the outer 1–3 cm of active xylem of 41 trees and shrubs, with two probes per tree. Species (number probed) were *A. rubrum* ($n = 4$), *B. lenta* ($n = 8$), *L. tulipifera* ($n = 4$), *Nyssa sylvatica* Marshall (Cornaceae) ($n = 4$), *Oxydendrum arboreum* DC. (Ericaceae) ($n = 5$), *Q. alba* ($n = 3$), and *R. maximum* ($n = 13$). These species together represented 87% of total stand basal area (S. Brantley, *unpublished data*). Probe length (1, 2, or 3 cm) was selected to permit sampling of at least 30% of the sapwood depth in all trees.

We monitored J_s from April 2011 to November 2011. Sap flux density was determined hourly from temperature differences (ΔT) between the upper and lower probes using a Granier-type power equation (Granier, 1985) with species-specific calibration coefficients derived on-site (Miniat et al. *unpublished data*). Maximum temperature differences were identified from the highest ΔT recorded during the previous week. J_s measurements were scaled to total sap flow ($g\ H_2O\ s^{-1}$) using known radial profiles for *A. rubrum*, *B. lenta*, *L. tulipifera* and *Q. alba* and a general radial profile for all other species (Ford and Vose, 2007). J_s was scaled to leaf-level transpiration (E_L, $mm\ h^{-1}$) using estimates of leaf area from each tree/shrub derived from species-specific allometric relationships between over-bark diameter at breast height (DBH) and leaf area (Martin et al., 1998; Santee, 1978; Santee and Monk, 1981).

Canopy stomatal conductance (G_S, $mol\ m^{-2}\ s^{-1}$) was derived from E_L according to $G_S = KE_L/D$, where D is vapor pressure deficit and K is a temperature dependent constant (Phillips & Oren, 1998). Conductance data were then filtered to remove data collected under limiting light (photosynthetically active radiation < 1400 $\mu mol\ m^{-2}\ s^{-1}$) and during low D ($D < 0.7$ kPa) when empirical relationships between G_S and D are not well constrained (Oren et al., 1999). The relationship between G_S and D was then examined independently for morning (<1200 EST) and afternoon (≥1200 EST) data using a boundary line analysis (Dye and Olbrich, 1993). The boundary line analysis was performed separately for the morning and afternoon data, and a simple regression between G_S and ln(D) was performed for each group.

3. Results

3.1. Wind regimes & the flux footprint

Wind predominantly flowed down-valley, originating from the SW (i.e., Sector 4, 230–310° from N, Fig. 1). However, the distribution of wind direction depended on the time of day. In early morning (midnight to 0500 h), wind was almost exclusively from Sector

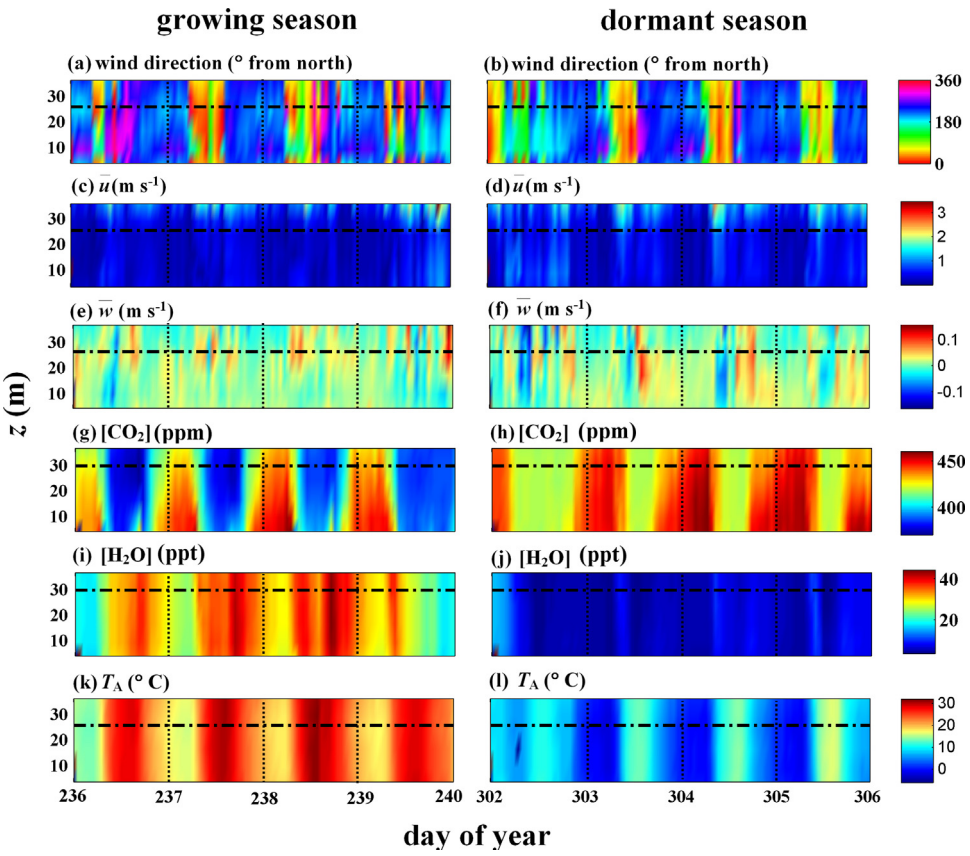

Fig. 3. Vertical within-canopy gradients of wind variables and scalar concentrations for four days during the growing season (left columns) and four days during the dormant season (right columns). Patterns observed during these time periods are typical of those observed throughout the study periods. Wind direction is shown in (a) and (b), the mean horizontal wind speed ($\bar{u}$) and vertical wind speed ($\overline{w}$) are shown in (c)–(f), and concentrations of CO_2, H_2O, and air temperature (T_a) are shown in panels (g)–(l). The horizontal dashed line indicates maximum canopy height.

4 (Fig. 1b); then, shortly before daybreak, wind direction often switched by ~180° to originate from Sector 2 (i.e., 40–85° from N, Figs. 1b and 3a,b). These up-valley winds originating from Sector 2 typically persisted until around noon, whereupon wind direction again switched to originate from Sector 4 (Figs. 1c,d and 3a,b). These patterns were observed in both the growing and dormant seasons (Fig. 3a and b).

Wind direction was usually uniform within and above the canopy, indicating coupling between above- and below-canopy flows; however, vertical gradients in wind direction occasionally developed and coincided with the occurrence of wind direction shifts between Sectors 2 and 4. Within-canopy gradients in horizontal wind speed were small, with $\overline{u(z)}$ varying by less than 0.1 m s^{-1}, on average, for z = 0 to h (Fig. 3c and d). The magnitude of $\overline{u(z)}$ was lower in the canopy air space relative to the above-canopy measurements in both the dormant and growing season (Fig. 3c and d), indicating that tree stems and branches function as momentum sinks even during leaf-off periods. The absolute magnitude of rotated vertical wind speed at z = 37 m was small, but tended to be positive during the daytime ($\overline{\langle w(z) \rangle} = 0.007$ m s^{-1}, where $\langle . \rangle$ denotes the average of all available runs) and negative at night ($\overline{\langle w(z) \rangle} = -0.004$ m s^{-1}). Both positive and negative gradients in $\overline{w(z)}$ were observed (Fig. 3e and f).

When wind was from Sector 4, the flux footprint was contained within forested land representative of the study ecosystem with very rare exceptions (Fig. 4a and b). During morning periods when wind originated from Sector 2, the footprint frequently (>80% of the time) included some areas of developed land located to the NE of the tower (Fig. 4d).

3.2. Scalar profiles, and storage and advection fluxes

Large nocturnal build-ups of CO_2 in the canopy airspace were observed during both the dormant and growing season (Fig. 3g and h). Nocturnal CO_2 concentrations were highest in the sub-canopy, promoting steep negative vertical gradients of CO_2 at night and in particular during early morning hours (i.e., 2400–0500, Fig. 3g and h). Throughout the canopy, CO_2 concentrations showed the fastest rate of increase early in the evening shortly before sunset (Fig. 3g and h); consequently, $F_{CO2,STOR}$ was positive in early evening ($\langle F_{C,STOR} \rangle \sim 2$ μmol m^{-2} s^{-1} and 5 μmol m^{-2} s^{-1} in the dormant and growing seasons, respectively, Fig. 5a and c). The temporal change in CO_2 concentration was most negative around sunrise (Fig. 3g and h), and consequently $F_{CO2,STOR}$ was negative in early morning ($\langle F_{C,STOR} \rangle \sim -2$ μmol m^{-2} s^{-1} and −5 μmol m^{-2} s^{-1} in the dormant and growing seasons, respectively, Fig. 5a–d).

Above-canopy vertical wind speed tended to be negative at night in all seasons (Fig. 3e and f). Because vertical advection fluxes were determined by the product of vertical wind speed and the scalar concentration gradient, $F_{C,VA}$ tended to be strongly positive in early morning (i.e., 2400–0500, Fig. 5a and c) when $\overline{w(z_r)}$ was <0 m s^{-1} and vertical gradients in CO_2 concentration were sharply negative. When a friction velocity filter (i.e., $u^* > 0.25$ m s^{-1}) was applied, the contribution $F_{C,VA}$ to the total ecosystem flux was minimized, though storage fluxes remained high (Fig. 5b and d).

The concentration of H_2O generally decreased in late evening and then increased in early morning (Fig. 3i and j), contributing to negative LE_{STOR} in early evening and positive LE_{STOR} in early morning. During the daytime, H_2O concentration reached a peak in early- to mid-afternoon, when LE_{STOR} was again positive

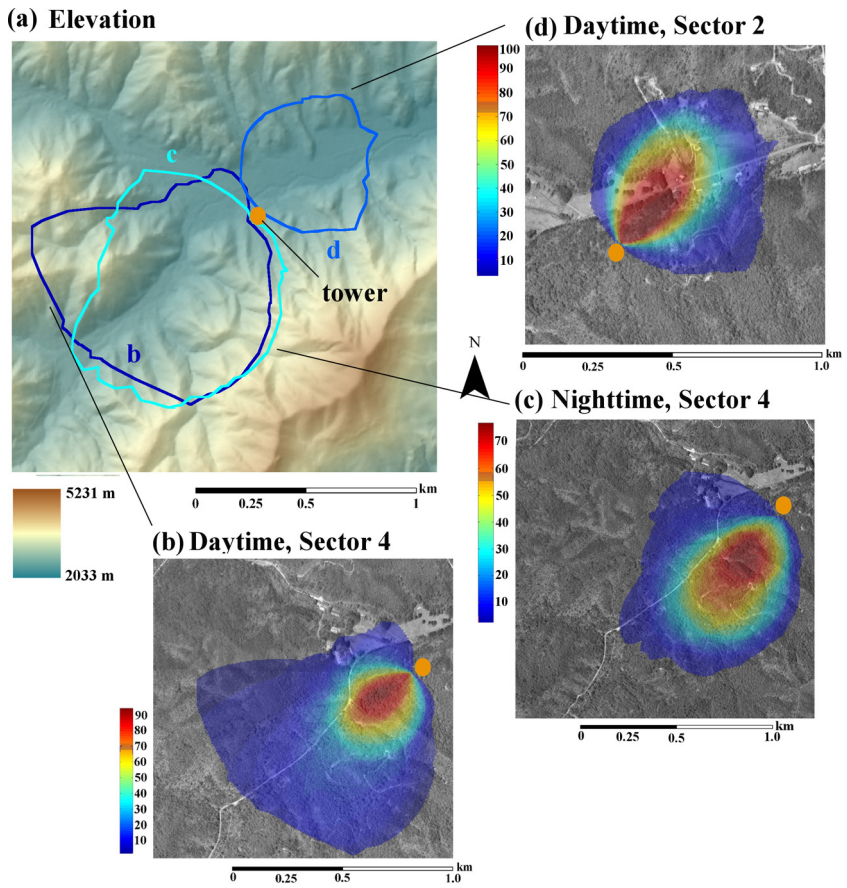

Fig. 4. Elevation in the vicinity of the flux tower is shown in (a). During daytime and nighttime periods when wind was from Sector 4 (i.e., 230–310° from north), the typical flux footprint overlaid forest areas within 0.5–1 km of the tower (panels b and d). During daytime periods when wind was from Sector 2 (i.e., 40–85° from north), the typical flux footprint frequently exceeded the dimensions of the study ecosystem (panel d). The colormaps in panels b–d show the frequency (expressed as a %) with which the footprint overlaid each parcel.

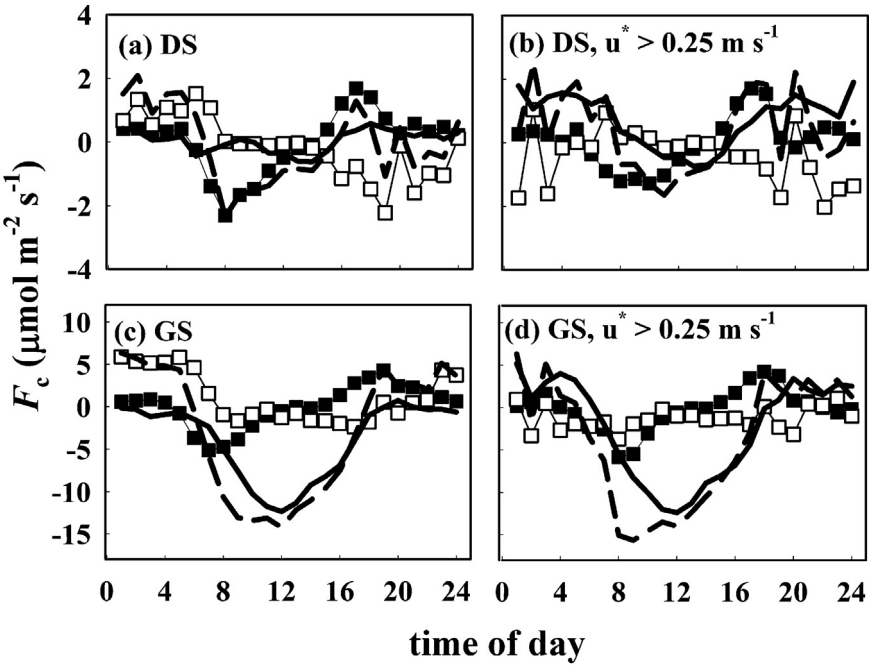

Fig. 5. The diurnal course of carbon fluxes, including turbulent fluxes (solid line), storage fluxes (solid squares), vertical advection fluxes (open squares) and their sum (dashed line). Data are shown separately for the dormant season (DS, a and b) and growing season (GS, c and d). The binned averages were calculated separately using all data (left column) and data collected when friction velocity (u^*) was greater than 0.25 m s^{-1} (right column).

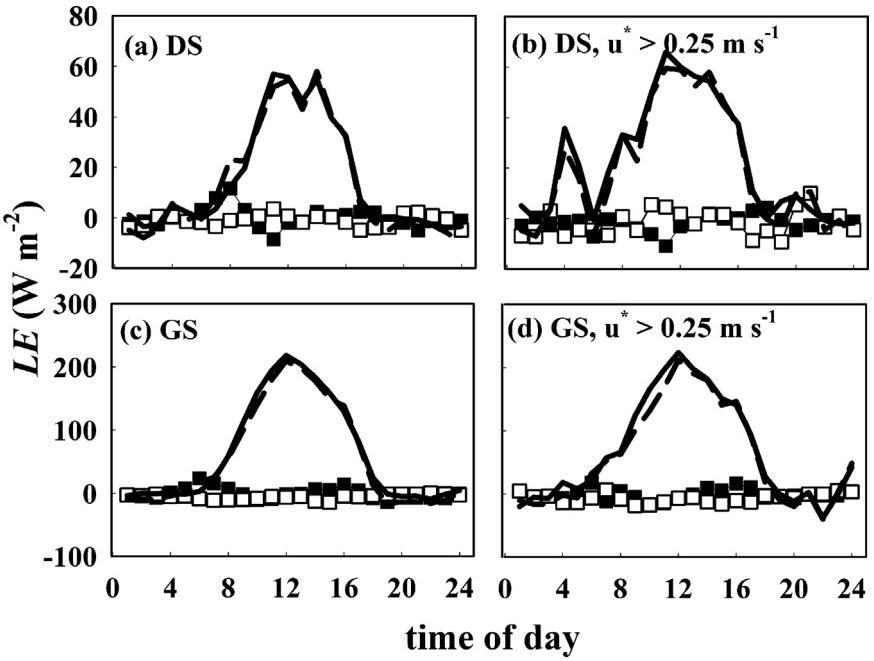

Fig. 6. Same as Fig. 5 but for latent heat fluxes.

and of similar magnitude as the early morning storage fluxes. However, the ratio of LE_{STOR} to the total ecosystem *LE* flux was small during daytime periods (Fig. 6) as compared to nighttime periods. Because temperature usually reached a local minimum shortly before sunrise and a maximum in the afternoon (Fig. 3k and l), H_{STOR} was typically positive from sunrise to about 1400 hours (Fig. 7), and negative or near zero otherwise. Vertical gradients in H_2O and air temperature were small relative to the gradients in CO_2 (Fig. 3g–l); consequently $F_{V,LE}$ and $F_{V,H}$ were a small component of the total ecosystem flux of latent and sensible heat (Figs. 5 and 6), respectively. Applying a friction velocity filter produced little change in the magnitudes of storage fluxes or vertical advection fluxes of latent or sensible heat (Figs. 5 and 6).

3.3. Temperature sensitivity of ecosystem respiration

The temperature sensitivity of RE_1, representing F_C^* measurements when $F_{C,EC}$ was near zero, did not agree well with the model of Eq. (5) ($r^2 = 0.26$, Fig. 8); the rate of increase in RE_1 with T_a under these conditions was not monotonic, with a local maximum occurring around $T_a = 20\,^{\circ}C$. Agreement between the model and RE_2 (which assumes a positive relationship between $F_{C,HA}$ and $F_{C,VA}$, see methods for details) was worse ($r^2 = 0.12$, Fig. 8). However, when *RE* was augmented with an assumed $F_{C,HA} = -0.5F_{C,VA}$ (i.e., RE_3), agreement with the model improved considerably ($r^2 = 0.67$, Fig. 8). Furthermore, RE_3 was similar in magnitude to RE_4, which was estimated using the measured sum of $F_{C,EC} + F_{C,STOR}$ when $F_{C,VA}$ was near zero. RE_4 also agreed well with the model ($r^2 = 0.81$). The close

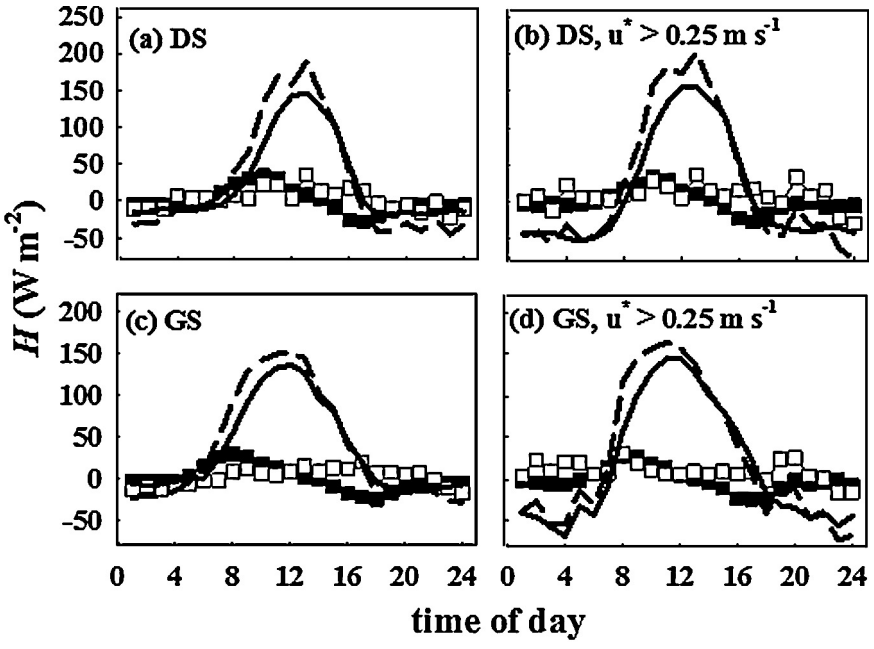

Fig. 7. Same as Fig. 5 but for sensible heat fluxes.

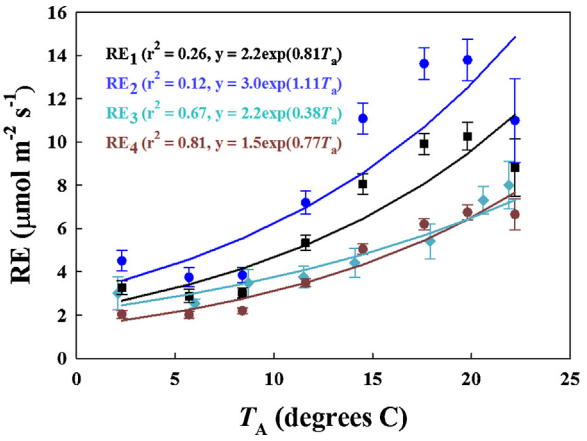

Fig. 8. The relationship between nocturnal ecosystem respiration (RE) and air temperature (T_a) estimated from binned averages of T_a using four approaches to estimating the respiration fluxes: (1) RE estimated from F_C^* collected when measured $F_{C,EC}$ was near zero (RE1); (2) RE estimated as the sum of RE1 + 0.5$F_{C,VA}$, reflecting an assumed positive correlation between horizontal and vertical advection fluxes (RE2), (3) RE estimated as the sum of RE1 − 0.5$F_{C,VA}$, reflecting an assumed negative correlation between horizontal and vertical advection fluxes (RE3), and (4) RE estimated from F_C^* collected when measured $F_{C,VA}$ was near zero (RE4). The lines show the model of Eq. (5) fitted to each dataset.

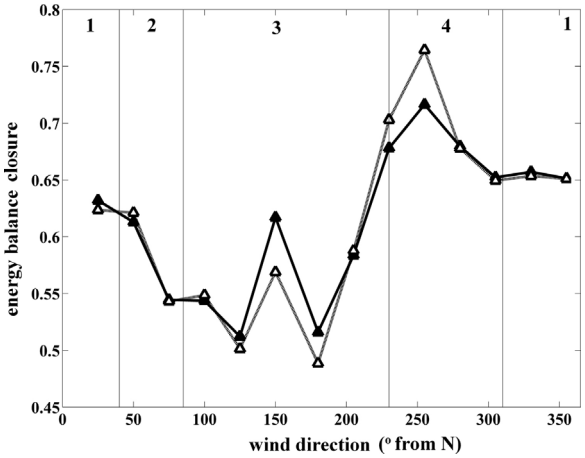

Fig. 10. Energy balance closure as a function of wind direction. Daytime data are represented with closed symbols, and nighttime data are represented with open symbols. The numbers at the top indicate the wind sector.

agreement between RE_3, RE_4, and the model of Eq. (5) suggest that during nocturnal periods, $F_{C,HA}$ and $F_{C,VA}$ are negatively related, and that minimizing data to those collected when $F_{C,VA}$ is near zero will also minimize the contribution of $F_{C,HA}$ to F_C.

3.4. Flux profiles

Agreement between growing season fluxes measured by the two above-canopy, open-path systems was best when wind originated from Sector 4 (Fig. 9). This was true for carbon, latent heat, and sensible heat fluxes regardless of time of day. Correcting the flux profile records for changes in storage and vertical advection between the two measurement heights improved carbon flux agreement slightly (Fig. 9a); but, had little effect on *LE* and *H* agreement (Fig. 9b and c). When wind was from Sector 4, corrected carbon fluxes agreed to within 1 μmol m^{-2} s^{-1} on average (corresponding to a relative error of <10%); latent heat fluxes agreed to within 10 W m^{-2} on average (corresponding to a relative error of <7%); and sensible heat fluxes agreed to within 4 W m^{-2} on average (corresponding to a relative error of <3%). When wind was from Sector 2, the difference in carbon flux between the two profile systems (ΔF_c) was large for daytime periods (2–3 μmol m^{-2} s^{-1}, Fig. 8a). For all fluxes, agreement between the two systems was poor when wind originated from Sectors 1 or 3, as expected.

3.5. Energy balance

Energy balance closure was highest when wind originated from Sector 4 (Fig. 10). In this case, the EBR metric approached 0.8. EBR was lowest when wind originated from Sector 3 (EBR ~ 0.55); and, EBR was relatively low when wind originated from Sectors 1 and

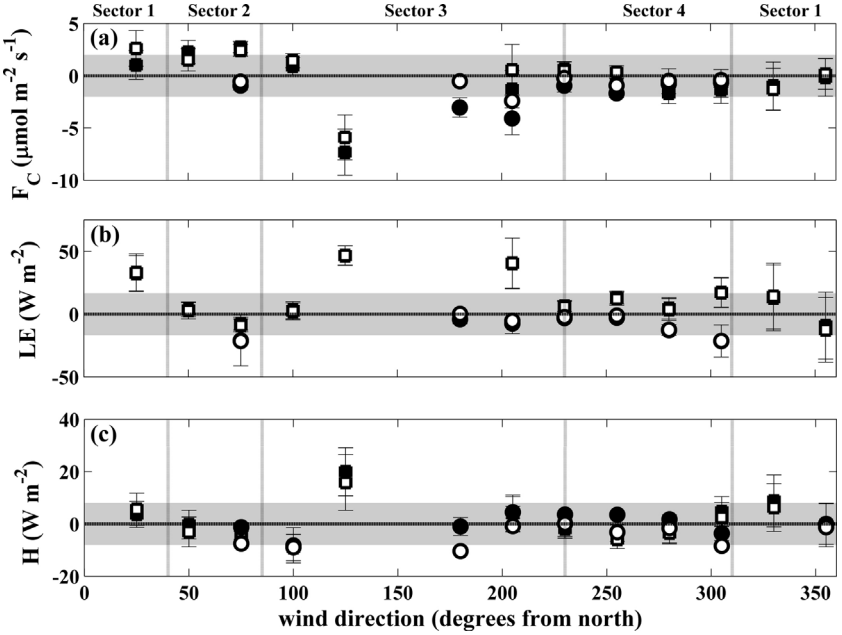

Fig. 9. The difference in CO_2 fluxes (a), latent heat fluxes (b), and sensible heat fluxes (c) measured by the two flux profile systems located at 33 and 37 m from August–December, 2011. Data are shown separately for differences in turbulent fluxes only (closed symbols), and differences in turbulent + vertical advection + storage fluxes (open symbols). Daytime data are shown with squares, and nighttime data are shown with circles. The vertical dashed lines delineate the four wind sectors.

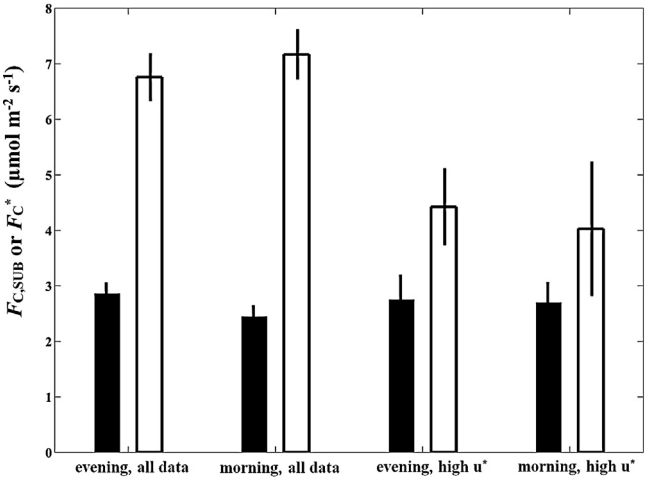

Fig. 11. The sub-canopy CO_2 flux ($F_{C,SUB}$ solid bars) and the sum of turbulent, vertical advection, and storage fluxes measured at the top of the canopy (F_C^*, open bars) for evening (sunset–2400) and morning (000–0500) periods using all available data, and data when friction velocity (u^*) is greater than 0.25 m s^{-1}.

2 (EBR = 0.55–0.65). Overall, even when wind originated from Sector 4, energy balance ratio was low when compared to other flux sites (see Wilson et al., 2002), where energy balance closure often exceeds 80%.

3.6. Comparison between above- and below-canopy CO_2 fluxes

When all available data were considered, the nocturnal CO_2 flux measured with the sub-canopy EC (i.e., $F_{C,SUB}$) system was lower than F_C^* measured above the canopy (Fig. 11). The ratio of $F_{C,SUB}$ to F_C^* was larger in early morning ($F_{C,SUB}$:F_C^* = 0.42, 000–0500 h) as compared to late evening ($F_{C,SUB}$:F_C^* = 0.34, sunset–2400 h). When data were filtered to remove measurements collected during low turbulence (i.e., when u^* measured above the canopy exceeded 0.25 m s^{-2}), $F_{C,SUB}$ and F_C^* were similar during evening periods and early morning ($F_{C,SUB}$:F_C^* = 0.67 and 0.62, respectively, Fig. 11).

3.7. Sap flux in morning as compared to afternoon periods

We found that the relationship between G_S and D ($G_S = m \ln(D) + b$) determined from a boundary line analysis during high light conditions was statistically indistinguishable for morning and afternoon periods (Fig. 12). The ratio m/b was 0.55 and 0.52 for morning and afternoon data, respectively, consistent with previous work (Oren et al., 1999) and predictions from ecological theory (Katul et al., 2009).

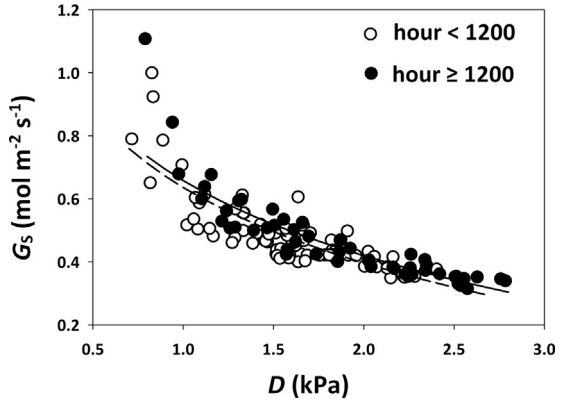

Fig. 12. The relationship between canopy stomatal conductance (G_S) and vapor pressure deficit (D) determined from sap flux data. The relationships developed for morning data (open circles, dashed line) and afternoon data (closed circles, solid line) are statistically indistinguishable (p = 0.91).

4. Discussion

The new flux monitoring tower at the Coweeta Hydrologic Laboratory is located in complex and heterogeneous terrain (Fig. 4), and a significant contribution of horizontal and vertical advection to total ecosystem fluxes of mass and energy was anticipated. Given the cost and difficulties in measuring horizontal advection flux in particular (Aubinet, 2008; Feigenwinter et al., 2010a), our principal objective was to interpret data collected from the singe flux monitoring tower to characterize the advection flux regime, so that data collected when advection fluxes are significant may be removed from the data record and gapfilled. While the flux regime observed here is likely to be highly site specific, the general approach may nonetheless be extended to other sites where advection is suspected to represent a significant contribution to total ecosystem fluxes.

Our results suggest that positive vertical advection of CO_2 is a prominent feature of this study site from approximately midnight to sunrise (Fig. 5), when wind was predominantly from the SW (i.e., downslope). The topographical slope in this direction is mild (<10%) and the wind tends to follow the topography (Fig. 1a). Nonetheless the persistent occurrence of negative vertical wind speed (after the planar-fit coordinate rotation was applied) in early morning periods (Fig. 3e–h) is indicative of subsidence of air into the canopy airspace – a hallmark of drainage flow regimes (Feigenwinter et al., 2010b; Lee, 1998; Turnipseed et al., 2003). The development of positive vertical advection fluxes of CO_2 (i.e., $F_{C,VA}$) is consistent with the development of drainage flows and indicates a convergence situation (using the classification scheme of Aubinet, 2008). Horizontal advection of CO_2 (i.e., $F_{C,HA}$) was not directly measured at the site; however, an exponential relationship between ecosystem respiration and temperature was only recovered when $F_{C,HA}$ was negatively related to $F_{C,VA}$, or when data were filtered to remove significant contributions from $F_{C,VA}$ (Fig. 8). We note that a pattern of positive $F_{C,VA}$ coupled with negative $F_{C,HA}$ is not without precedent (Aubinet, 2008; Feigenwinter et al., 2004), and this conclusion is further supported by comparing the magnitude of sub-canopy CO_2 flux (i.e., $F_{C,SUB}$) to the sum of turbulent, storage, and vertical advection carbon fluxes (i.e., F_C^*) measured with the tower. The average difference between F_C^* and $F_{C,SUB}$ decreases (Fig. 11) when data are filtered to remove the contribution of $F_{C,VA}$ to F_C^*, which suggests the existence of a negative $F_{C,HA}$ in the unfiltered data. A pattern of $F_{C,VA} > 0$, $F_{C,HA} < 0$, and $|F_{C,HA}| < |F_{C,VA}|$ at night would suggest a decrease in source intensity (i.e., respiration) along the streamline (Aubinet, 2008). In this site, a decrease in source intensity could be realized if drainage flows lead to the accumulation of cool air near the valley base where the tower is located.

We note that this analysis cannot rule out the existing of some component of $F_{C,HA}$ that is not related to $F_{C,VA}$. However, if the models for RE_3 and RE_4 are applied to estimate RE for the entire year, the resulting annual fluxes (1858 and 1942 g C m^{-2}) are within the range of annual RE estimates derived from eddy covariance measurements, which rarely exceed 2000 g C m^{-2} in temperate forest ecosystems (Lasslop et al., 2010; Falge et al., 2001). By contrast, annual RE fluxes derived from models RE_1 and RE_2 are 2756 and 3645 g C m^{-2} are considerably higher than those previously reported for other temperate forests. Thus, the existence of a large and persistent $F_{C,HA}$ is unlikely at this site. In any event, confirmation that $F_{C,VA} > 0$, $F_{C,HA} < 0$, and $|F_{C,HA}| < |F_{C,VA}|$ could come from a detailed comparison of eddy covariance carbon fluxes to those

estimated by scaling plot- and tree-level measurements to the ecosystem, which is an ongoing effort at the study site.

From approximately sunrise to noon, wind direction switched to originate from the NE; this pattern is also characteristic of drainage mountain flows, as shallow up-valley and anabatic winds may develop in morning periods concurrent with the break-cup of capping inversions and the development of a convective mixed layer (Stull, 1988). When wind originates from the NE, the flux footprint exceeds the dimensions of the study ecosystem (Fig. 4), and agreement between F_C* measured at different points about the canopy was poor (Fig. 9), reflecting the existence of horizontal advection or horizontal flux divergence. The energy balance ratio was also poor when wind originated from the NE (Fig. 10), which could reflect the influence of advection fluxes as well as a mis-match between the flux footprint and the footprint of the net radiometer. In any event, data collected when wind originated from the NE are unlikely to be representative of scalar fluxes from the forest ecosystem surrounding the tower.

A small amount of data was collected when wind originated from Sectors 1 and 3, in which case the angle of attack was large and diverged considerably from the local slope (Fig. 1). Previous work has shown that vertical wind speed is a difficult variable to measure and a source of large uncertainty in the determination of turbulent and vertical advection flux estimates, particularly when w is large (Gash and Dolman, 2003; Kochendorfer et al., 2012; Nakai et al., 2006). Thus, a priori, we expected uncertain flux measurements collected when wind originated from Sectors 1 and 3. This expectation was confirmed by poor agreement in fluxes measured at two points above the canopy and poor energy balance closure when wind originated from Sectors 1 and 3.

In summary, data from our single tower showed that the contribution of advection to the net ecosystem exchange of mass and energy at this site are minimized from noon to midnight provided wind originated from the SW (i.e., Sector 4), and that reliable annual estimates of ecosystem exchange will require the gapfilling of other data (representing roughly 50% of the data record). The need to gapfill the majority of nocturnal flux data is a frequently occurring challenge at existing flux sites, including sites on relatively flat terrain (Reichstein et al., 2005; van Gorsel et al., 2009). The need to gapfill the majority of morning (i.e., sunrise to noon) data is, to our knowledge, a challenge specific to our site, though results from sap flux data show that physiological functioning is similar in morning and afternoon approaches, supporting the use of a daytime gapfilling approach that relies largely on afternoon data. The gapfilling approach is discussed in more detail below, following an examination of sources of error in the datasets.

4.1. Difficulties in measuring w and the relevance of these challenges to this analysis

Turbulent and vertical flux estimates are sensitive to errors in vertical wind speed. Errors in w may be related to (a) static offsets representing persistent instrument biases related to the electronic functioning of anemometers (Heinesch et al., 2007; Wilczak et al., 2001), (b) dynamic offsets representing flow distortions around anemometer struts or the tower itself (Heinesch et al., 2007; Kochendorfer et al., 2012), (c) tilt-angles related to sonic orientations that are not precisely vertical with respect to gravitational potential (Paw U et al., 2000; Wilczak et al., 2001), and (d) the choice and application of the coordinate rotation scheme (Paw U et al., 2000; Wilczak et al., 2001). In general, errors and uncertainties increase when the wind angle of attack approach the large values observed in this study (Kochendorfer et al., 2012), and the vertical velocity measurements presented here are acknowledged to be uncertain estimates. By adopting a data screening approach that relies on the removal of data collected when the total ecosystem scalar fluxes were not well represented by the sum of turbulent and storage fluxes, we may avoid correcting an already uncertain turbulent flux measurement with imprecise measurements of advection fluxes. Thus, errors in w are limited to affecting the turbulent flux terms. In a previous study, we show that errors in w related to static and dynamic instrument offsets and tilt-angles contribute to minimal biases in measured scalar fluxes provided conditions are sufficiently well mixed (Novick et al., 2013). The effect of systematic biases in w related to the coordinate rotation scheme on measured fluxes could be identified by comparisons of tower-based flux measurements of CO_2 and LE to those derived from independent biometric measurements, which we stress is the focus of ongoing work at the site.

4.2. Energy balance closure

In most eddy covariance applications, the energy balance is not fully closed. In a synthesis relying on 50 site-years of data from 22 sites representing a range of climate and vegetation characteristics, Wilson et al. (2002) found that energy balance closure estimated using the EBR approach ranged from 0.34 to 1.69, with a mean of 0.84. In this context, EBR at our study site is relatively low (Fig. 10). Even when wind originated from Sector 4 (i.e., the most favorable regime) during the daytime (when advection fluxes are expected to be low), daytime energy balance closure was on the order of 0.7–0.8. This imbalance could reflect a contribution to the total ecosystem water or heat flux from horizontal advection, or uncertainty in the vertical advection flux estimates. This imbalance could also reflect uncertainties in the energy budget variables that are unrelated to advection fluxes. For example, heat storage in above-ground biomass has been shown to be a significant contribution to the total ecosystem energy budget (Lindroth et al., 2010), and could be high in this dense forest ecosystem where basal area is close to 30 m^2 ha^{-1}. Additionally, our study site is characterized by a spatially heterogeneous understory of Rhododendron (*R. maximum*), which forms a dense, evergreen sub-canopy 2–4 m tall. It is possible that heat storage fluxes within Rhododendron canopies differs from those in open areas of the sub-canopy due to differences in aerodynamic conductance and micro-climate. Testing this hypothesis is a focus of ongoing research in the study site.

4.3. Implications for gapfilling strategies

Vertical advection fluxes appeared close to midnight and persisted through much of the early morning (Fig. 5). The onset of vertical advection fluxes a few hours after sunset, as was observed here, is a common problem at many eddy covariance sites, and standardized procedures exist to filter and gapfill nocturnal flux data collected in the presence of vertical and horizontal advection (van Gorsel et al., 2009). Indeed, when data were screened in a manner suggested by the van Gorsel study (i.e., RE_4, or data collected within a few hours after sunset, when vertical advection fluxes are low), agreement between nocturnal RE and air temperature closely matched predictions from a model (Fig. 8), and preliminary estimates of annual RE using this approach ($\sim$1950 g C m^{-2}) are well within the range of those estimated in other temperature deciduous forests.

The need to reject much of the data collected from sunrise – noon, when wind originated from Sector 2, is a more novel problem. Established approach for gapfilling eddy covariance flux data include look-up tables and similar methodologies that rely on averages of acceptable data collected under similar meteorological conditions (Falge et al., 2001; Novick et al., 2013; Reichstein et al., 2005) or the application of simple models that relate acceptable measured fluxes to meteorological drivers (Lasslop et al., 2010; Stoy et al., 2006). Both of these approaches are reasonable approaches

for gapfilling the missing morning data at our site, but their success will require that physiological functioning is similar in the morning and afternoon, or that diel differences in the driving variables controlling mass and energy exchange are well represented in the model or look-up table. One variable that is an important control on both carbon and water vapor exchange is canopy stomatal conductance (i.e., G_S). Our analysis using sap flux data collected within the vicinity of the tower showed that the relationship between G_S and vapor pressure deficit was statistically indistinguishable between morning and afternoon periods (Fig. 12). In other forest ecosystems, hysteresis in the relationship between G_S and VPD has been observed that is linked to soil moisture and VPD limitations to plant functioning (Ford et al., 2004; Phillips et al., 2003; Tuzet et al., 2003). As our study site receives nearly 2 m of rainfall a year, soil moisture will not often be limiting and VPD is not often high. Thus, for this site, using afternoon flux data to create look-up tables or simple models could be a reasonable strategy to gapfill the large amount of missing carbon and water vapor flux data in the morning.

5. Conclusions

Our analysis revealed that approximately 50% of data were collected during periods when vertical advection fluxes were observed, or when horizontal advection fluxes were inferred. During nocturnal periods in the early morning (2400–0600), large positive vertical advection fluxes were observed, which were likely driven by drainage flows and accompanied by negative horizontal advection fluxes. During morning daylight periods (0600–1200), flux footprint analyses coupled with observations of vertical flux divergence suggest the presence of horizontal advection fluxes driven by anabatic flows over heterogeneous terrain. Broadly speaking, results from this analysis agree with other studies showing that wind regime patterns and their associated advection fluxes are highly site-specific (Aubinet et al., 2010; Yi et al., 2005). Nonetheless, the approach outlined here, which relies on observation streams that may be collected from a single flux tower (i.e., vertical advection flux measurements, vertical flux profile measurements, wind profile measurements, flux footprint estimates, and energy balance closure) could be generally applied to other sites where the advection flux regime needs to be characterized. Taken together, these observations are sufficient to characterize patterns of vertical advection, and to infer the likely magnitude and direction of horizontal advection, with the exception of horizontal advection fluxes in the sub-canopy that are decoupled from above-canopy advection regimes. The presence of such a decoupled sub-canopy horizontal advection flux may be detected by comparing eddy covariance CO_2 fluxes to independent estimates of the components of ecosystem carbon fluxes (i.e., chamber-based soil respiration fluxes, stem respiration measurements, etc.), which is an ongoing effort at this site. In summary, the flux measurement approach described here is well suited to capture mid-day (noon) to late-evening fluxes (midnight) in this complex and heterogeneous environment. Our analysis highlight the additional need of future work at this and similar sites to incorporate gapfilling strategies to specifically account for fluxes during nighttime and morning hours.

Acknowledgements

We thank a number of individuals who assisted with data collection and analysis, including Chris Sobek, Neal Muldoon, Joe Davis, Randy Fowler, Stephanie Laseter, Bob McCollom, and Sander Denham. We thank Chris Oishi, Jielun Sun, and Asko Noormets for valuable comments on an earlier version of the manuscript. We are also grateful to Gaby Katul for providing valuable advice regarding experimental design. This document has been reviewed in accordance with U.S. Environmental Protection Agency policy and approved for publication. Mention of trade names or commercial products does not constitute endorsement or recommendation for use.

References

Aubinet, M., 2008. Eddy covariance CO(2) flux measurements in nocturnal conditions: an analysis of the problem. Ecological Applications 18 (6), 1368–1378.

Aubinet, M., Feigenwinter, C., Heinesch, B., Bernhofer, C., Canepa, E., Lindroth, A., Montagnani, L., Rebmann, C., Sedlak, P., van Gorsel, E., 2010. Direct advection measurements do not help to solve the night-time CO(2) closure problem: evidence from three different forests. Agricultural and Forest Meteorology 150 (5), 655–664.

Baldocchi, D., 2008. Breathing of the terrestrial biosphere: lessons learned from a global network of carbon dioxide flux measurement systems. Australian Journal of Botany 56 (1), 1–26.

Baldocchi, D.D., 2003. Assessing the eddy covariance technique for evaluating carbon dioxide exchange rates of ecosystems: past, present and future. Global Change Biology 9 (4), 479–492.

Baldocchi, D.D., Law, B.E., Anthoni, P.M., 2000. On measuring and modeling energy fluxes above the floor of a homogeneous and heterogeneous conifer forest. Agricultural and Forest Meteorology 102 (2–3), 187–206.

Baldocchi, D.D., Finnigan, J., Wilson, K., Paw, U., Falge, K.T.E., 1999. On measuring net ecosystem carbon exchange over tall vegetation on complex terrain. Boundary-Layer Meteorology 96, 257–291.

Detto, M., Montaldo, N., Albertson, J.D., Mancini, M., Katul, G., 2006. Soil moisture and vegetation controls on evapotranspiration in a heterogeneous Mediterranean ecosystem on Sardinia, Italy. Water Resources Research 42. (8).

Dye, P.J., Olbrich, B.W., 1993. Estimating transpiration from 6-year-old *Eucalyptus grandis* trees: development of a canopy conductance model and comparison with independent sap flux measurements. Plant, Cell and Environment 16, 45–53.

Falge, E., Baldocchi, D., Tenhunen, J., Aubinet, M., Bakwin, P., Berbigier, P., Bernhofer, C., Burba, G., Clement, R., Davis, K.J., Elbers, J.A., Goldstein, A.H., Grelle, A., Granier, A., Guomundsson, J., Hollinger, D., Kowalski, A.S., Katul, G., Law, B.E., Malhi, Y., Meyers, T., Monson, R.K., Munger, J.W., Oechel, W., Paw U, K.T., Pilegaard, K., Rannik, U., Rebmann, C., Suyker, A., Valentini, R., Wilson, K., Wofsy, S., 2002. Seasonality of ecosystem respiration and gross primary production as derived from FLUXNET measurements. Agricultural and Forest Meteorology 113 (1–4), 53–74.

Falge, E., Baldocchi, D., Olson, R., Anthoni, P., Aubinet, M., Bernhofer, C., Burba, G., Ceulemans, R., Clement, R., Dolman, H., Granier, A., Gross, P., Grunwald, T., Hollinger, D., Jensen, N.O., Katul, Gl., Keronen, P., Kowalski, A., Lai, C.T., Law, B.E., Meyers, T., Moncrieff, H., Moors, E., Munger, J.W., Pilegaard, K., Rannik, U., Rebmann, C., Suyker, A., Tenhunen, J., Tu, K., Verman, S., Vesala, T., Wilson, K., Wofsy, S., 2001. Gap filling strategies for defensible annual sums of net ecosystem exchange. Agricultural and Forest Meteorology 107 (1), 43–69.

Feigenwinter, C., Bernhofer, C., Eichelmann, U., Heinesch, B., Hertele, Janous, D., Kolle, O., Lagergren, F., Lindroth, A., Minerbi, S., Moderow, U., Mölder, M., Montagnani, L., Queck, R., Rebmann, C., Vestin, P., Yernaux, M., Zeri, M., Ziegler, W., Aubinet, M., 2008. Comparison of horizontal and vertical advective CO_2 fluxes at three forest sites. Agricultural and Forest Meteorology 148 (1), 12–24.

Feigenwinter, C., Bernhofer, C., Vogt, R., 2004. The influence of advection on the short term CO_2-budget in and above a forest canopy. Boundary-Layer Meteorology 113 (2), 201–224.

Feigenwinter, C., Molder, M., Lindroth, A., Aubinet, M., 2010a. Spatiotemporal evolution of CO_2 concentration, temperature, and wind field during stable nights at the Norunda forest site. Agricultural and Forest Meteorology 150 (5), 692–701.

Feigenwinter, C., Montagnani, L., Aubinet, M., 2010b. Plot-scale vertical and horizontal transport of CO_2 modified by a persistent slope wind system in and above an alpine forest. Agricultural and Forest Meteorology 150 (5), 665–673.

Foken, T., 2008. The energy balance closure problem: an overview. Ecological Applications 18 (6), 1351–1367.

Ford, C.R., Goranson, C.E., Mitchell, R.J., Will, R.E., Teskey, R.O., 2004. Diurnal and seasonal variability in the radial distribution of sap flow: predicting total stem flow in Pinus taeda trees. Tree Physiology 24 (9), 941–950.

Ford, C.R., Vose, J.M., 2007. *Tsuga canadensis* (L.) Carr. mortality will impact hydrologic processes in southern appalachian forest ecosystems. Ecological Applications 17 (4), 1156–1167.

Friend, A.D., Arneth, A., Kiang, N.Y., Lomas, M., Ogee, J., Rodenbeckk, C., Running, S.W., Santaren, J.D., Sitch, S., Viovy, N., Woodward, F.I., Zaehle, S., 2007. FLUXNET and modelling the global carbon cycle. Global Change Biology 13 (3), 610–633.

Gash, J.H.C., Dolman, A.J., 2003. Sonic anemometer (co)sine response and flux measurement I. The potential for (co)sine error to affect sonic anemometer-based flux measurements. Agricultural and Forest Meteorology 119 (3–4), 195–207.

Gockede, M., Rebmann, C., Foken, T., 2004. A combination of quality assessment tools for eddy covariance measurements with footprint modelling for the characterisation of complex sites. Agricultural and Forest Meteorology 127 (3–4), 175–188.

Granier, A., 1985. A new method of sap flow measurement in tree stems. Annals of Forest Science 42, 192–200.

Gu, L.H., Meyers, T., Pallardy, S.G., Hanson, P.J., Yang, B., Heuer, M., Hosman, K.P., Liu, Q., Riggs, J.S., Sluss, D., Wullschleger, S.D., 2007. Influences of biomass heat and

biochemical energy storages on the land surface fluxes and radiative temperature. Journal of Geophysical Research-Atmospheres 112 (D2), 11.
Heinesch, B., Yernaux, M., Aubinet, M., 2007. Some methodological questions concerning advection measurements: a case study. Boundary-Layer Meteorology 122 (2), 457–478.
Hsieh, C.I., Katul, G.G., Chi, T.W., 2000. An approximate analytical model for footprint estimation of scalar fluxes in thermally stratified atmospheric flows. Advances in Water Resources 23, 765–772.
Katul, G.G., Palmroth, S., Oren, R., 2009. Leaf stomatal responses to vapour pressure deficit under current and CO_2-enriched atmosphere explained by the economics of gas exchange. Plant Cell and Environment 32 (8), 968–979.
Kochendorfer, J., Meyers, T.P., Frank, J., Massman, W.J., Heuer, M.W., 2012. How well can we measure the vertical wind Speed? Implications for fluxes of energy and mass. Boundary-Layer Meteorology 145 (2), 383–398.
Krinner, G., Viovy, N., de Noblet-Ducoudre, N., Ogee, J., Polcher, J., Friedlingstein, P., Ciais, P., Sitch, S., Prentice, I.C., 2005. A dynamic global vegetation model for studies of the coupled atmosphere-biosphere system. Global Biogeochemical Cycles 19. (1).
Kutsch, W.L., Kolle, O., Rebmann, C., Knohl, A., Ziegler, W., Schulze, E.D., 2008. Advection and resulting CO(2) exchange uncertainty in a tall forest in central Germany. Ecological Applications 18 (6), 1391–1405.
Lasslop, G., Reichstein, M., Papale, D., Richardson, A.D., Arneth, A., Barr, A., Stoy, P., Wohlfahrt, G., 2010. Separation of net ecosystem exchange into assimilation and respiration using a light response curve approach: critical issues and global evaluation. Global Change Biology 16 (1), 187–208.
Law, B.E., Falge, E., Gu, L., Baldocchi, D.D., Bakwin, P., Berbigier, P., Davis, K., Dolman, A.J., Falk, M., Fuentes, J.D., Goldstein, A., Granier, A., Grelle, A., Hollinger, D., Janssens, I.A., Jarvis, P., Jensen, N.O., Katul, G., Mahli, Y., Matteucci, G., Meyers, T., Monson, R., Munger, W., Oechel, W., Olson, R., Pilegaard, K., Paw U, K.T., Thorgeirsson, H., Valentini, R., Verma, S., Vesala, T., Wilson, K., Wofsy, S., 2002. Environmental controls over carbon dioxide and water vapor exchange of terrestrial vegetation. Agricultural and Forest Meteorology 113 (1–4), 97–120.
Lee, X.H., 1998. On micrometeorological observations of surface-air exchange over tall vegetation. Agricultural and Forest Meteorology 91 (1–2), 39–49.
Leuning, R., Zegelin, S.J., Jones, K., Keith, H., Hughes, D., 2008. Measurement of horizontal and vertical advectlion of CO(2) within a forest canopy. Agricultural and Forest Meteorology 148 (11), 1777–1797.
Lindroth, A., Molder, M., Lagergren, F., 2010. Heat storage in forest biomass improves energy balance closure. Biogeosciences 7 (1), 301–313.
Loescher, H.W., Law, B.E., Mahrt, L., Hollinger, D.Y., Campbell, J., Wofsy, S.C., 2006. Uncertainties in, and interpretation of, carbon flux estimates using the eddy covariance technique. Journal of Geophysical Research-Atmospheres 111 (D21).
Martin, J.G., Kloeppel, B.D., Schaefer, T.L., Kimbler, D.L., McNulty, S.G., 1998. Aboveground biomass and nitrogen allocation of ten deciduous southern Appalachian tree species. Canadian Journal of Forest Research-Revue Canadienne De Recherche Forestiere 28 (11), 1648–1659.
Massman, W.J., 2000. A simple method for estimating frequency response corrections for eddy covariance systems. Agricultural and Forest Meteorology 104 (3), 185–198.
Massman, W.J., 2001. Reply to comment by Rannik on "A simple method for estimating frequency response corrections for eddy covariance systems". Agricultural and Forest Meteorology 107 (3), 247–251.
Moderow, U., Aubinet, M., Feigenwinter, C., Kolle, O., Lindroth, A., Molder, M., Montagnani, L., Rebmann, C., Bernhofer, C., 2009. Available energy and energy balance closure at four coniferous forest sites across Europe. Theoretical and Applied Climatology 98 (3–4), 397–412.
Nakai, T., van der Molen, M.K., Gash, J.H.C., Kodama, Y., 2006. Correction of sonic anemometer angle of attack errors. Agricultural and Forest Meteorology 136 (1–2), 19–30.
Novick, K., Walker, J.T., Chan, W.S., Schmidt, A., Sobek, C., Vose, J.M., 2013. Eddy covariance measurements with a new fast-response, enclosed-path analyzer: spectral characteristics and cross-system comparisons. Agricultural and Forest Meteorology 181, 17–32.
Oncley, S.P., Foken, T., Vogt, R., Kohsiek, W., DeBruin, H.A.R., Bernhofer, C., Christen, A., van Gorsel, E., Grantz, D., Feigenwinter, C., Lehner, I., Liebethal, C., Liu, H., Mauder, M., Pitacco, A., Ribeiro, L., Weidinger, T., 2007. The Energy Balance Experiment EBEX-2000. Part I: Overview and energy balance. Boundary-Layer Meteorology 123 (1), 1–28.
Oren, R., Sperry, J.S., Katul, G.G., Pataki, D.E., Ewers, B.E., Phillips, N., Schafer, K.V.R., 1999. Survey and synthesis of intra- and interspecific variation in stomatal sensitivity to vapour pressure deficit. Plant Cell and Environment 22 (12), 1515–1526.
Paw, U., Baldocchi, K.T., Meyers, D.D., Wilson, T.P.K.B., 2000. Correction of eddy-covariance measurements incorporating both advective effects and density fluxes. Boundary-Layer Meteorology 97 (3), 487–511.
Phillips, N.G., Ryan, M.G., Bond, B.J., McDowell, N.G., Hinckley, T.M., Cermak, J., 2003. Reliance on stored water increases with tree size in three species in the Pacific Northwest. Tree Physiology 23 (4), 237–245.
Phillips, N., Oren, R., 1998. A comparison of daily representations of canopy conductance based on two conditional time-averaging methods and the dependence of daily conductance on environmental factors. Annales Des Sciences Forestieres 55 (1–2), 217–235.
Rebmann, C., Gockede, M., Foken, T., Aubinet, M., Aurela, M., Berbigier, P., Bernhofer, C., Buchmann, N., Carrara, A., Cescatti, A., Ceulemans, R., Clement, R., Elbers, J.A., Granier, A., Grunwald, T., Guyon, D., Havrankova, K., Heinesch, B., Knohl, A., Laurila, T., Longdoz, B., Marcolla, B., Markkanen, T., Miglietta, F., Moncrieff, J., Montagnani, L., Moors, E., Nardino, M., Ourcival, J.M., Rambal, S., Rannik, U., Rotenberg, E., Sedlak, P., Unterhuber, G., Vesala, T., Yakir, D., 2005. Quality analysis applied on eddy covariance measurements at complex forest sites using footprint modelling. Theoretical and Applied Climatology 80 (2–4), 121–141.
Reichstein, M., Rey, A., Freibauer, A., Tenhunen, J., Valentini, R., Banza, J., Casals, P., Cheng, Y.F., Grunzweig, J.M., Irvine, J., Joffre, R., Law, B.E., Loustau, D., Miglietta, F., Oechel, W., Ourcival, J.M., Pereira, J.S., Peressotti, A., Ponti, F., Qi, Y., Rambal, S., Rayment, M., Romanya, J., Rossi, F., Tedeschi, V., Tirone, G., Xu, M., Yakir, D., 2003. Modeling temporal and large-scale spatial variability of soil respiration from soil water availability, temperature and vegetation productivity indices. Global Biogeochemical Cycles 17 (4).
Reichstein, M., Falge, E., Baldocchi, D., Papale, D., Aubinet, M., Berbigier, P., Bernhofer, C., Buchmann, N., Gilmanov, T., Granier, A., Grunwald, T., Havrankova, K., Ilvesniemi, H., Janous, D., Knohl, A., Laurila, T., Lohila, A., Loustau, D., Matteucci, G., Meyers, T., Miglietta, F., Ourcival, J.M., Pumpanen, J., Rambal, S., Rotenberg, E., Sanz, M., Tenhunen, J., Seufert, G., Vaccari, F., Vesala, T., Yakir, D., Valentini, R., 2005. On the separation of net ecosystem exchange into assimilation and ecosystem respiration: review and improved algorithm. Global Change Biology 11 (9), 1424–1439.
Reichstein, M., Beer, C., 2008. Soil respiration across scales: the importance of a model-data integration framework for data interpretation. Journal of Plant Nutrition and Soil Science 171, 344–354.
Santee, W.R., 1978. A dimensional analysis of Eastern Hemlock (*Tsuga Canadensis*). University of Georgia, Athens, Georgia, pp. 96.
Santee, W.R., Monk, C.D., 1981. Stem diameter and dry weight relationships in *Tsuga canadensis* (L.) Carr. Bulletin of the Torrey Botanical Club 108, 320–323.
Schmid, H.P., Grimmond, C.S.B., Cropley, F., Offerle, B., Su, H.B., 2000. Measurements of CO_2 and energy fluxes over a mixed hardwood forest in the mid-western United States. Agricultural and Forest Meteorology 103 (4), 357–374.
Staebler, R.M., Fitzjarrald, D.R., 2004. Observing subcanopy CO_2 advection. Agricultural and Forest Meteorology 122 (3–4), 139–156.
Stoy, P.C., Katul, G.G., Siqueira, M.B.S., Juang, J.-Y., Novick, K.A., McCarthy, H.R., Oishi, A.C., Uebelherr, J.M., Kim, H.S., Oren, R., 2006. Separating the effects of climate and vegetation on evapotranspiration along a successional chronosequence in the southeastern US. Global Change Biology 12 (11), 2115–2135.
Stull, R.B., 1988. An Introduction to Boundary Layer Meteorology, 13. Springer, Dordrecht, The Netherlands, pp. 670.
Sun, J.Ll., Burns, S.P., Delany, A.C., Oncley, S.P., Turnipseed, A.A., Stephens, B.B., Lenschow, D.H., LeMone, M.A., Monson, R.K., Anderson, D.E., 2007. CO2 transport over complex terrain. Agricultural and Forest Meteorology 145 (1–2), 1–21.
Turnipseed, A.A., Anderson, D.E., Blanken, P.D., Baugh, W.M., Monson, R.K., 2003. Airflows and turbulent flux measurements in mountainous terrain Part 1. Canopy and local effects. Agricultural and Forest Meteorology 119 (1–2), 1–21.
Tuzet, A., Perrier, A., Leuning, R., 2003. A coupled model of stomatal conductance, photosynthesis and transpiration. Plant Cell and Environment 26 (7), 1097–1116.
van Gorsel, E., Delpierre, N., Leuning, R., Black, A., Munger, J.W., Wofsy, S., Aubinet, M., Feigenwinter, C., Beringer, J., Bonal, D., Chen, B.Z., Chen, J.Q., Clement, R., Davis, K.J., Desai, A.R., Dragoni, D., Etzold, S., Grunwald, T., Gu, L.H., Heinesch, B., Hutyra, L.R., Jans, W.W.P., Kutsch, W., Law, B.E., Leclerc, M.Y., Mammarella, I., Montagnani, L., Noormets, A., Rebmann, C., Wharton, S., 2009. Estimating nocturnal ecosystem respiration from the vertical turbulent flux and change in storage of CO_2. Agricultural and Forest Meteorology 149 (11), 1919–1930.
Vose, J.M., Bolstad, P.V., 2006. Biotic and abiotic factors regulating forest floor CO_2 flux across a range of forest age classes in the southern Appalachians. Pedobiologia 50 (6), 577–587.
Webb, E.K., Pearman, G.I., Leuning, R., 1980. Correction of flux measurements for density effects due to heat and water-vapor transfer. Quarterly Journal of the Royal Meteorological Society 106 (447), 85–100.
Wilczak, J.M., Oncley, S.P., Stage, S.A., 2001. Sonic anemometer tilt correction algorithms. Boundary-Layer Meteorology 99 (1), 127–150.
Williams, M., Richardson, A.D., Reichstein, M., Stoy, P.C., Peylin, P., Verbeeck, H., Carvalhais, N., Jung, M., Hollinger, D.Y., Kattge, J., Leuning, R., Luo, Y., Tomelleri, E., Trudinger, C.M., Wang, Y.P., 2009. Improving land surface models with FLUXNET data. Biogeosciences 6 (7), 1341–1359.
Wilson, K., Goldstein, A., Falge, E., Aubinet, M., Baldocchi, D., Berbigier, P., Bernhofer, C., Ceulemans, R., Dolman, H., Field, C., Grelle, A., Ibrom, A., Law, B.E., Kowalski, A., Meyers, T., Moncrieff, J., Monson, R., Oechel, W., Tenhunen, J., Valentini, R., abd Verma, S., 2002. Energy balance closure at FLUXNET sites. Agricultural and Forest Meteorology 113 (1–4), 223–243.
Yi, C.X., Anderson, D.E., Turnipseed, A.A., Burns, S.P., Sparks, J.P., Stannard, D.I., Monson, R.K., 2008. The contribution of advective fluxes to net ecosystem exchange in a high-elevation, subalpine forest. Ecological Applications 18 (6), 1379–1390.
Yi, C.X., Monson, R.K., Zhai, Z.Q., Anderson, D.E., Lamb, B., Allwine, G., Turnipseed, A.A., Burns, S.P., 2005. Modeling and measuring the nocturnal drainage flow in a high-elevation, subalpine forest with complex terrain. Journal of Geophysical Research-Atmospheres 110 (D22).
Yi, C., Davis, K.J., Bakwin, P.S., Berger, B.W., Marr, L.C., 2000. Influence of advection on measurements of the net ecosystem-atmosphere exchange of CO_2 from a very tall tower. Journal of Geophysical Research-Atmospheres 105 (D8), 9991–9999.